MĀPAN-Journal of Metrology Society of India
https://doi.org/10.1007/s12647-021-00481-x

ORIGINAL PAPER

Evaluation and Control Perceptive of VSM-Based Multilevel PV-STATCOM for Distributed Energy System

M. P. Thakre* and N. Kumar

K. K. Wagh Institute of Engineering Education and Research, Nashik, Maharashtra, India

Received: 08 March 2021 / Accepted: 03 June 2021

Abstract: With the increasing penetration of distributed energy resources into the power grid, the intermittency property of non-conventional sources has made it compulsory to propose an appropriate controlling system so as to have maximum utilization of the clean energy resources. The idea of utilizing a photovoltaic (PV) system inverter integrated with grid as STATCOM is termed as PV-STATCOM has been used to demonstrate the behaviour of two different controllers: $d-q$ frame PLL-based and VSM-based controllers. Both controllers are compared to a PV-STATCOM system integrated into the power grid, which is simulated at various electrical contingencies to determine their dependability and proficiency. The article starts with a brief explanation of virtual synchronous machine (VSM) and its area of utilization. The study system with PLL-based and VSM-based controller is then simulated with 3-level and 5-level multilevel inverters separately for sudden load changes, fault analysis, FFT analysis and voltage sag compensation in MATLAB/Simulink. Finally, the results from these cases are evaluated, confirming that the VSM-based controller outperforms the $d-q$ frame PLL-based controller in terms of measuring voltage transients during sudden load changes, voltage and current magnitudes during ground faults, and exhibiting low THD levels.

Keywords: Virtual synchronous machine (VSM); Phase-locked loop (PLL); PV-STATCOM; Distributed energy resources (DERs); Multilevel converter

1. Introduction

The day to day increase in power demand and the adverse effect on the environment and scarcity of conventional energy resources has led the energy sector to shift its focus from fossil fuels to non-conventional energy resources like wind, solar and hydro energies which are available in abundance and free of cost in nature. Thus, to make use of these clean resources, a proper high efficiency system must be employed to fulfil the power demands. Various approaches have been proposed by researchers in recent years for integrating non-conventional energy resources into the power grid and providing auxiliary support from the distributed energy resources. A multi-level controlling scheme of a three-phase grid-connected PV system and its detailed mathematical model used as a distributed generator (DG) has been proposed [1]. A proposal to regulate the reactive power supplies from non-conventional energy resources to the power grid has been proposed [2]. Power quality is an important characteristic in renewable DG because current electrical loads are mostly non-linear and more sensitive to power quality disturbances. Therefore, there is always a necessity to introduce power quality improvement techniques. Due to an increase in non-linear loads, there is a rapid rise in the harmonic injection in the power system which has an adverse effect on residential and commercial loads [3, 4]. In order to mitigate the harmonic distortion, R–C filters are also utilized in distributed energy resources [5]. In order to reduce power quality issues and reactive power, flexible alternating current devices (FACTS) have been taken into usage. STATCOM has shown better results than other FACTS devices [6–9]. DSTATCOM is used at the distribution level to mitigate the harmonic distortions injected by the high penetration of renewable energy resources into the grid in [10, 11]. Power quality at the point of common coupling (PCC) can be improved by controlling the grid interfaced inverter of the DER system with the appropriate controller [12].

In this article, a PV system is considered which is being integrated with the electric grid. PV-STATCOM is a

*Corresponding author, E-mail: mohanthakre@gmail.com

Published online: 14 June 2021

unique concept of using the PV system's inverter as STATCOM for voltage regulation during both night time and daytime [13, 14]. The PV system produces active power during the daytime whereas it remains idle during the night time due to non-availability of solar energy. A PV-STATCOM uses the whole inverter capacity in the night which is left after active power generation during the day to achieve various STATCOM functionalities. PV-STATCOM can improve the power transfer capability limits of the interconnected transmission [15]. During night time, the whole inverter capacity is used for STATCOM functionality. When a critical disturbance occurs during the day, the inverter stops its active power production operation temporarily (for a small time) and gives away its inverter capacity for STATCOM functionality [16].

In the PV-STATCOM system for controlling the active and reactive powers, the current controller in the $d-q$ frame is utilized with a separate synchronizing unit called phase-locked loop (PLL) [17]. Researchers have proposed various designing and controlling techniques for PLL in [18–22] and the comparison of different PLL topologies has been discussed in [23]. The patented concept of utilizing synchronous machine emulation for the controlling of converters connected to the renewable energy resources that are integrated with the electric grid was proposed by Lennart Harnefors [24]. Later on, this emulation of synchronous machine was termed as virtual synchronous machine (VSM) [25, 26], virtual synchronous generator (VSG) [27, 28] or synchronverter [29, 30] by various researchers. The control designs of VSM-based controller are proposed by taking the advantage of the synchronization capability of synchronous machine without incorporating a special synchronization unit, PLL [31, 32]. The VSM-based controller is also incorporated in the DER system for the mitigation of voltage and frequency fluctuations [33, 34] and it has superior operation over the PLL-based controller when there are sudden load changes in the power system [35].

As the power generation using a PV system is DC, an inverter is required to convert it into AC. Researchers have proposed various inverter topologies for optimal utilization of power at an economical cost. A 15-level inverter configuration which has 6 two-quadrant switches, 3 isolated switches and 4 four-quadrant switches with fault tolerance capability for PV application has been proposed in [36]. Due to the intermittent behaviour of the PV system, power quality problems arise. A cascaded 5-level inverter system controlled by closed loop artificial neural network (ANN) has the tendency to reduce the harmonic injection due to PV system [37, 38]. The utilization of multilevel inverters for reactive power compensation has increased in recent years as they have finer harmonic attributes and excellent dynamic performance than multiphase inverters [39, 40]. Multilevel inverters are mostly utilized in PV-STATCOM systems like 5-level cascaded H-bridge multilevel inverter [41, 42] to reduce the total harmonic distortion (THD) significantly.

Most of the researchers have controlled the PV-STATCOM system with the help of a current control loop incorporated with $d-q$ frame PLL for synchronizing the PV-STATCOM system with the grid. However, the performance of PLL is always in doubt when there are more numbers of inverters present in the system. The novel concept of utilizing VSM for controlling the PV-STATCOM has been proposed in this article. Two different approaches for controlling the PV-STATCOM system are considered here, one with a PLL-based controller and the other with a VSM-based controller to have comparative analysis between them. Both the controllers for inverters have been simulated with sudden load changes, fault analysis, voltage sag compensation and THD analysis for 3-level and 5-level diode clamped multilevel inverters. The novelty of the VSM-based controller is done on the basis of the PLL-based controller's harmonics compensation [5], synchronization unit [17] and controller complexity [35].

The novelty and original contribution of the paper are as follows:

- The proposed controller for the PV-STATCOM system uses the concept of virtual synchronous machine (VSM) for integrating and synchronizing the non-conventional source of electric energy with the power grid.
- The proposed controller has the synchronization characteristics of a conventional synchronous machine, unlike the existing controller which employs a separate unit called phase-locked loop (PLL) for synchronization purpose.
- The proposed controller is simple in design whereas the PLL based controller is complex and needs tuning of the PLL, which is a time-consuming process.
- Virtual impedance in VSM is employed to restrict the harmonics generated by the converter and can reject or suppress the harmonics coming from the system, ensuring the power system is immune to harmonic perturbations without the need of having separate filters, especially employed for harmonics compensation.

The article will continue as follows: Section 2 will give a detailed description of virtual synchronous machine (VSM). Section 3 will consist of $d-q$ frame PLL-based and VSM-based controller study systems to be studied. Section 4 gives the simulated results of different cases performed on the study systems, Sect. 5 will provide the brief discussion on the results obtained from these cases performed and finally the conclusion in Sect. 6.

2. Virtual Synchronous Machine (VSM)

The idea of VSM in the context of smart grid is to emulate the behaviour of synchronous machines for distributed energy resources (DERs) integrated with the electric grid. The dynamic behaviour of synchronous machines is emulated into the mathematical modelling of VSM so as to provide auxiliary services like damping oscillation, reactive power control and inertia emulation with power electronic controller [33]. The primary objective of the VSM-based controller is to replace the $d-q$ frame controller which relies on a phase locked loop unit for synchronization, whereas the VSM-based controller prevails naturally in harmony with the electric system. This property of VSM prevents the system from getting into instability and improves the transient response when contingencies occur.

In a power system with excitation control and speed governor, the synchronous machine (SM) offers a perfect highlight to accomplish the system operations. A synchronous machine with its dynamic characteristics permits the accessibility of varying reactive and active powers, featuring the rotating mass and damping windings effects and the dependency of the grid frequency on the rotor speed, and as well as steady state operation in VSM. The main portion of VSM is the usage of the swing formula to maintain synchronism with the system.

$$\frac{\mathrm{d}\delta}{\mathrm{d}t} = \omega - \omega n \tag{1}$$

$$M\frac{\mathrm{d}^2\delta}{\mathrm{d}t^2} = P_{\mathrm{dc}} - P_{\mathrm{ac}} - D(\omega - \omega n) \tag{2}$$

$$M\frac{\mathrm{d}\omega}{\mathrm{d}t} = P_{\mathrm{dc}} - P_{\mathrm{ac}} - D(\omega - \omega n) \tag{3}$$

where δ is the power angle, ω_{n} is the grid frequency, ω is the detected frequency, M is the angular momentum, P_{ac} is the output active power from AC end of the inverter, P_{dc} is the input active power from DC end of the inverter and D is the damping coefficient, D is termed as virtual damping coefficient and M as virtual angular momentum and in the VSM context. Figure 1 represents the fundamental control block diagram of a VSM based controller. The VSM conception can be described by taking an analogy of a standard synchronous machine (SM) with an imaginary shaft rotating at ω rad/s angular frequency which is speeded up by P_{dc} and slowed down by P_{ac}. In the case ω is greater than grid frequency, ω_{n}, δ will become larger, thus increasing P_{ac} and then the value of ω will be decreased by the fluctuation in the output and input powers. In balanced mode, both the powers would be the same and thus making the system and grid frequency equal, thus showing perfect synchronism between the system and grid.

With virtual inertia in VSM, the PV-STATCOM system inherently gets synchronized with the electric grid correctly in case there are any changes in the frequency without risking the synchronization of the system. The synchronous machine rotor inertia is emulated by combining the energy storage with the converters. Due to better control performance, the VSM-based control is successfully applied to multilevel converters, voltage source converters (VSC), and energy storage systems.

Virtual impedance in VSM is employed to restrict the harmonics generated by the converter and can reject or suppress the harmonics coming from the system, ensuring the power system is immune to harmonic perturbations. This makes the VSM-based STATCOM less sensitive to voltage and power fluctuations induced by the grid or non-conventional energy sources, achieving improved voltage control and introducing better synchronization characteristics than the traditional $d-q$ frame based PLL controller.

The VSM-based controller thus does not require a separate synchronization unit like PLL; it is inherently in coordination with the power system. The VSM-based controller is simpler in design compared to the $d-q$ frame PLL-based controller which is very complex. It is a time-consuming process of tuning the PLL parameters, thus the non-requirement of PLL in VSM-based controller gives an upper hand over the conventional controller.

3. Study System Analysis

Figure 2 shows the study system which is being used to analyse the performance of $d-q$ frame PLL-based controller and VSM-based controller. The study system includes a solar PV array with 88 parallel strings, each string with 7 modules connected in series, and an output voltage of 481 V that is integrated with a 25 kV electric grid via a voltage source inverter that acts as a STATCOM; thus, the entire system, including the PV array and inverter, is referred to as PV-STATCOM. The voltage source inverter (VSI) is modelled such that it is utilized as a STATCOM with equivalent impedance of Z_{s} which constitutes the filters and transformer, an output current, i and voltage of v. The power grid is designed as a voltage-source of impedance Z_{g} composed of a transformer and filters, with a rated value of v_{g} and a grid current of i_{g}. The study system is being simulated in MATLAB/Simulink using both PLL-based and VSM-based controllers. Figure 3 shows the system developed in MATLAB/Simulink.

- Study System 1: PLL-Based PV-STATCOM Controller

Figure 4 shows the $d-$q frame PLL-based controller which is connected to the PV-STATCOM system. The

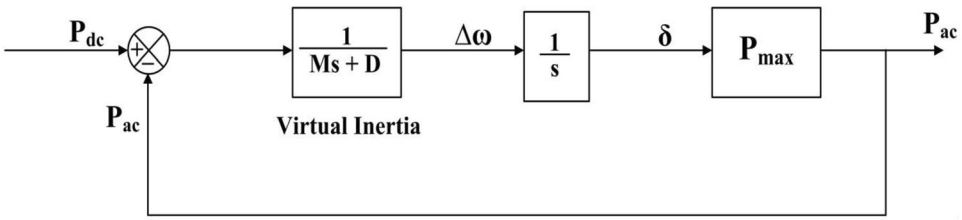

Fig. 1 Block diagram of virtual synchronous machine (VSM) controller

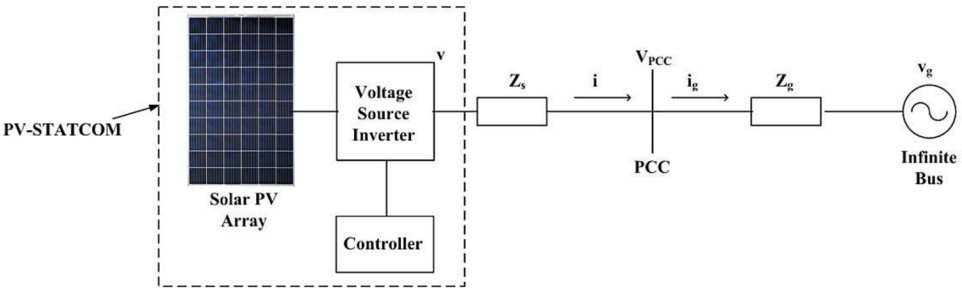

Fig. 2 Study system of PV-STATCOM

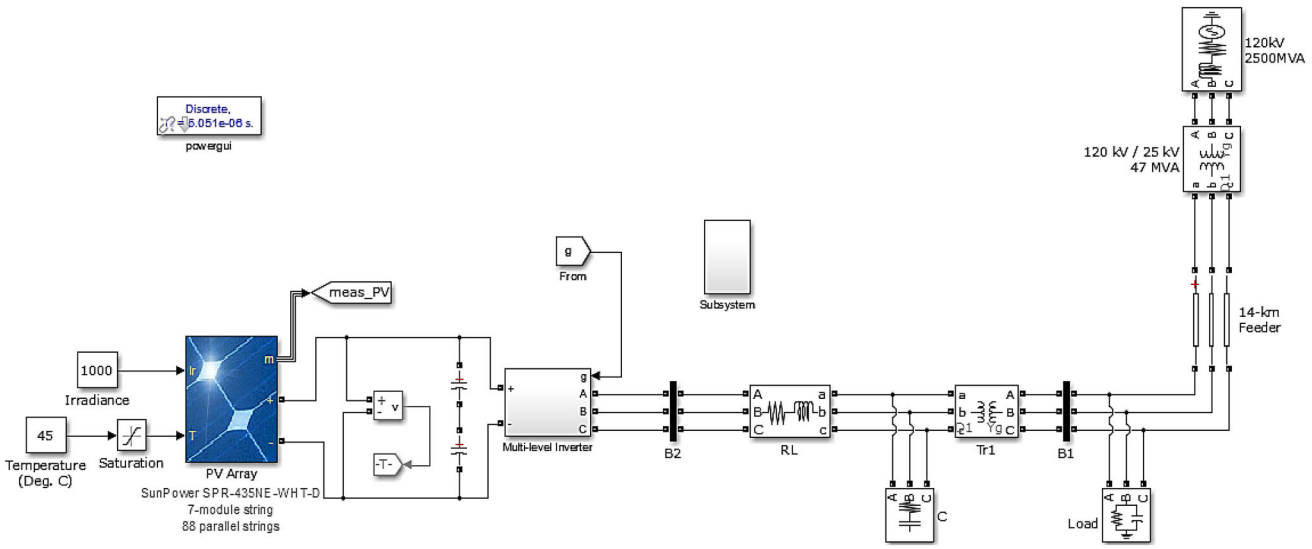

Fig. 3 System in MATLAB/Simulink

controller for the PV-STATCOM system offers reactive power compensation during night-time and active power control during daytime [14]. A $d-q$ frame PLL based control is used to keep synchronism with the point of common coupling (PCC). With a current controller utilized in dq0 frame the voltage-based control is employed. Q and P are the reactive and real powers which are needed to be managed. The real power, P is controlled by DC-link voltage control. The reference current, d and q frame components are obtained using P and Q power signals with the help of Eq. (4).

$$\begin{pmatrix} i_{\mathrm{d}}^{*} \\ i_{\mathrm{q}}^{*} \end{pmatrix} = \frac{1}{v_{\mathrm{gd}}^{2} + v_{\mathrm{gq}}^{2}} \begin{pmatrix} v_{\mathrm{gd}} & -v_{\mathrm{gq}} \\ v_{\mathrm{gq}} & v_{\mathrm{gd}} \end{pmatrix} \begin{pmatrix} P^{*} \\ Q^{*} \end{pmatrix} \tag{4}$$

The switching pulses for VSI are generated using $d-q$ frame upper and lower current control loops. The active power is injected into the electric grid using an upper current loop and adjusts the DC link voltage with the help of two PI controllers. The reactive power flow is controlled using the lower current loop through the inverter. The current component is rendered into active and reactive components and is compared with the reference signals obtained from Eq. (4) to generate an error signal. Using this error signal, the switching pulses for the inverter are generated.

- Study System 2: VSM-Based PV-STATCOM Controller

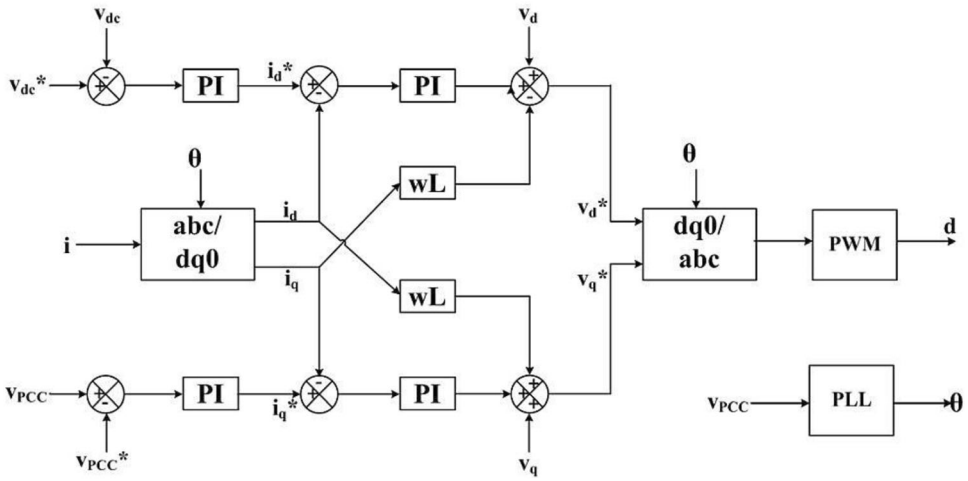

Fig. 4 $d-q$ frame phase-locked loop (PLL) based controller

Figure 5 depicts the VSM-based controller which is connected to the PV-STATCOM system. The VSM utilises the swing equation which can be seen in the part which incorporates virtual inertia, M and virtual damping coefficient, D. The value of virtual angular momentum, M is taken ($5 \times 10^{-3} \times \omega_n$) and that of virtual damping coefficient, D is taken ($1 \times \omega_n$). The need for a separate synchronization unit (like PLL) is eliminated in this controller as it gives the phase and frequency information of a virtual rotational mass which is utilized in synchronism with the electric grid in steady mode with a phase difference represented as power angle. There are 2 voltage control loops: one to control the dc-link voltage, V_{dc} error via a PI controller.

The other voltage control loop is utilized to manage the value of the PCC bus voltage, Vpcc. A PI controller is used to control the error in the magnitude of the PCC bus voltage, Vpcc, which generates virtual emf, E* Back emf, e in abc frame is rendered from virtual EMF, E * with the help of an oscillator having a phase angle of θ which is obtained from the virtual inertia. The STATCOM terminal voltage, v is subtracted with the back emf, e and the resultant is then divided by the virtual impedance which consists of virtual inductance, L and virtual resistance, R of values 50 and $0.1/\pi$ respectively, to generate the reference current, i^*. In the VSM controller to control the compensating current, the current loop is realized inside the $d-q$ frame which produces the duty cycle, d for the inverter.

4. Simulation Results

(a) Simulation Results for Sudden Load Changes

The given study system has been simulated in MATLAB/Simulink for sudden load changes for both PLL and VSM based controllers for PV-STATCOM system in [35] and are included here as well.

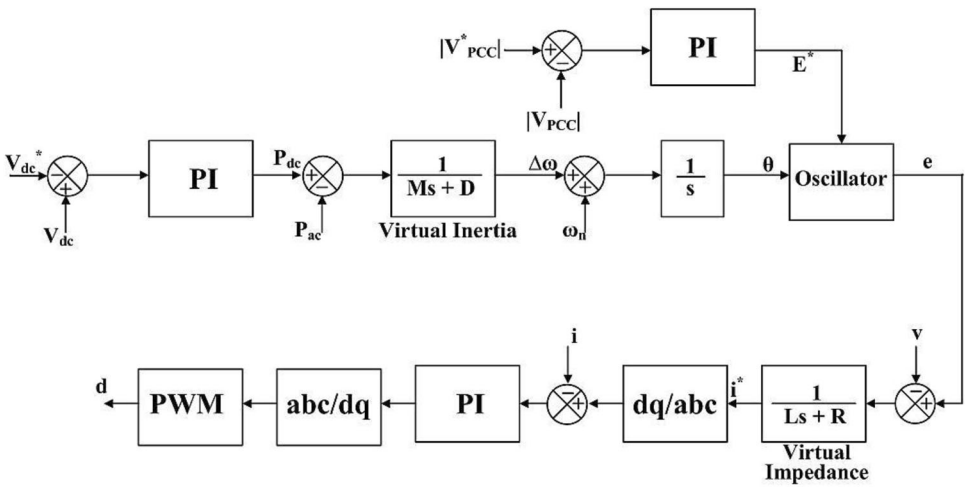

Fig. 5 Virtual synchronous machine (VSM) based controller

1. PLL-Based Controller

Figure 6 depicts the voltage profile at PCC when a PLL-based controller is connected to the PV-STATCOM system. An extra variable load of 8 MVAR and 12 MW is added at time, $t = 0.2$ s. The additional burden is then varied to 5 MVAR and 7 MW at $t = 0.3$ s, once more the load is varied to a magnitude of 10 MVAR and 15 MW at $t = 0.4$ s; and in the end it is reduced to 2 MVAR and 4 MW at $t = 0.5$ s. Figure 7 represents the enlarged perspective of voltage transients at the PCC because of sudden variation in load values. The $d-q$ frame controller exhibits large variations in the voltage contour and these voltage transients cross the limit set by IEEE std. 1547.2 [43] for voltage transients. These voltage transients can have an adverse effect on the electrical system as the voltage transients settling time are quite high and can have severe effects on the system. Figure 8 shows the active power which shows spikes at the time when the loads are suddenly changed and Fig. 9 shows the reactive power injected or absorbed by PV-STATCOM in order to compensate for the power demands to keep the system at a steady state.

2. VSM-Based Controller

Figure 10 depicts the voltage profile at PCC when the VSM-based controller is connected to the PV-STATCOM system. At time $t = 0.2$ s, an extra variable load of 8 MVAR and 12 MW is added to the system, which is then varied to 5 MVAR and 7 MW at $t = 0.3$ s, 10 MVAR and 15 MW at $t = 0.4$ s, and finally 2 MVAR and 4 MW at $t = 0.4$ s. Figure 11 depict the enlarged perspective of voltage transients occurred at PCC due to variation in the load values. The results obtained for the VSM-based controller have voltage transients of lower magnitude than the $d-q$ frame controller and have voltage transients magnitude well within the limits specified by IEEE std. 1547.2 [43]. The settling time of the transients is considerably lower and hence, if the system is affected by these transients, then there would be minimal damage to the system. Figure 12 shows the active power which shows spikes at the time when the loads are suddenly changed and Fig. 13 shows the reactive power injected or absorbed by PV-STATCOM in order to compensate for the power demands to keep the system at a steady state.

Figure 14 shows the comparison of frequency profiles for sudden load changes for both the controllers. It is observed from the comparison of frequencies that the frequency increases when load is decreased and frequency decreases when load is increased. However, the point that needs to be pointed out here is that when the VSM based controller is connected, the grid frequency tends to vary very close to the rated frequency (which is 50 Hz) than the PLL based controller's grid frequency response.

(b) Fault Analysis for 3-Level and 5-Level Converter for PV-STATCOM System

The PV-STATCOM system is connected with 3-level and 5-level multilevel controllers separately and their current and voltage profiles at PCC are analysed with all the ground faults in electrical systems at different fault resistances.

1. 3 Level Multilevel Converter with PLL-Based and VSM-Based Controller

(i) LG Fault

Figure 15 shows the behaviour of PCC voltage and PCC current when a 3-level converter is connected to both the controllers for simple LG fault for different fault resistance values. According to IEEE std. 1159, the voltage transients during fault conditions must be between 110 and 180% of

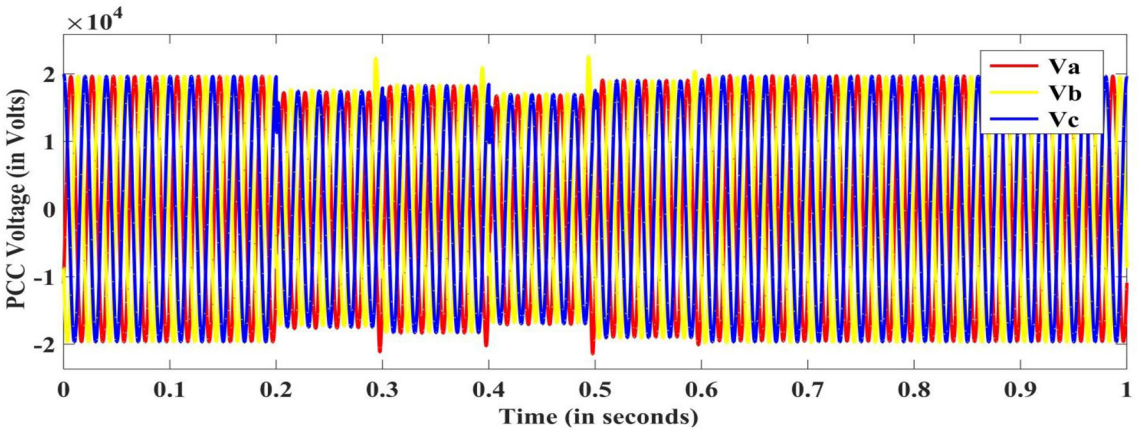

Fig. 6 PLL-based controller voltage profile for sudden load changes [35]

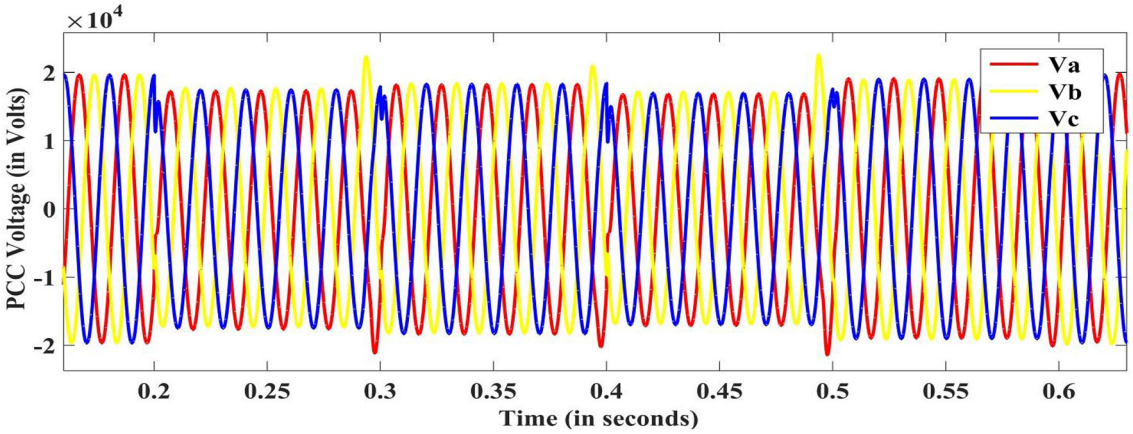

Fig. 7 Enlarged view of voltage profile for sudden load changes [35]

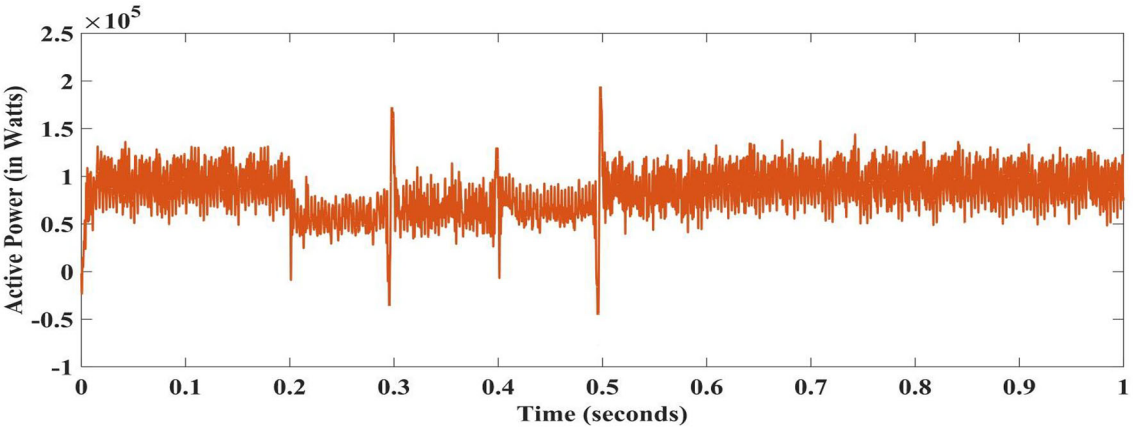

Fig. 8 Active power profile for PLL-based controller for sudden load changes

Fig. 9 Reactive power profile for PLL-based controller for sudden load changes

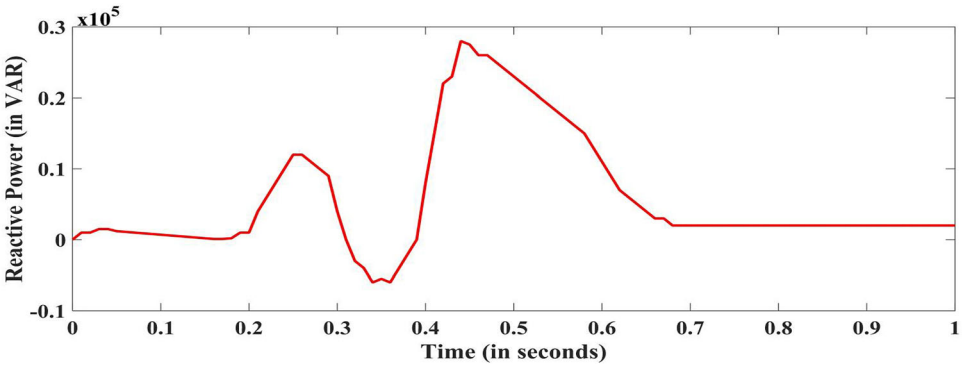

nominal voltage [44]. Both the controllers satisfy the IEEE standards and are well within the limits.

(ii) LLG Fault

Figure 16 depicts the behaviour of PCC current and PCC voltage when a 3-level converter is connected to both the controllers for LLG fault for different fault resistance values. Both the controllers satisfy the IEEE standards and are well within the limits.

(iii) LLLG Fault

Figure 17 shows the behaviour of PCC voltage and PCC current when a 3-level converter is connected to both the controllers for LLLG fault for different fault resistance

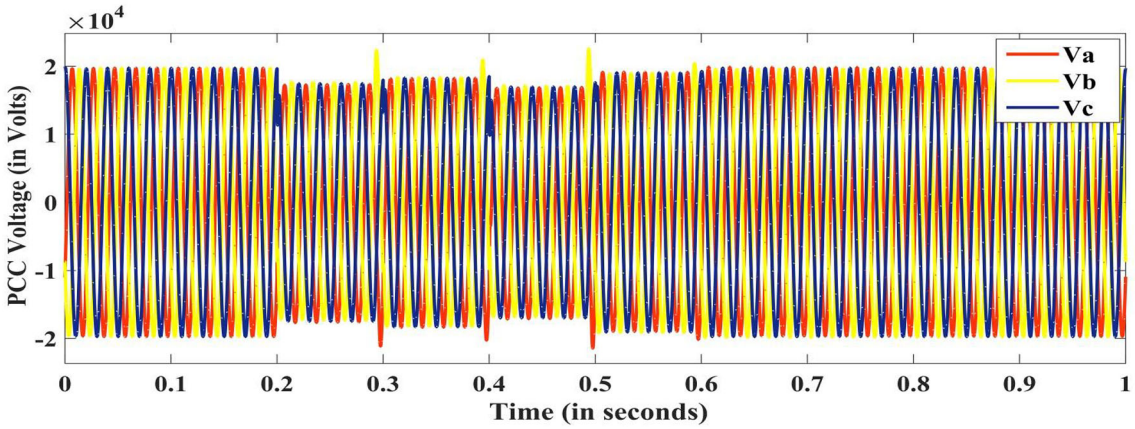

Fig. 10 VSM-based controller voltage profile for sudden load changes [35]

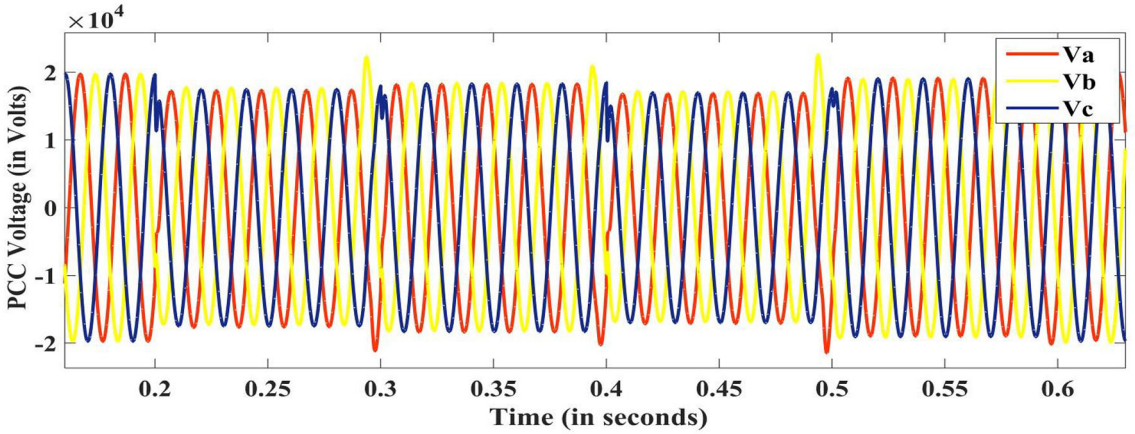

Fig. 11 Enlarged view of voltage profile for sudden load changes [35]

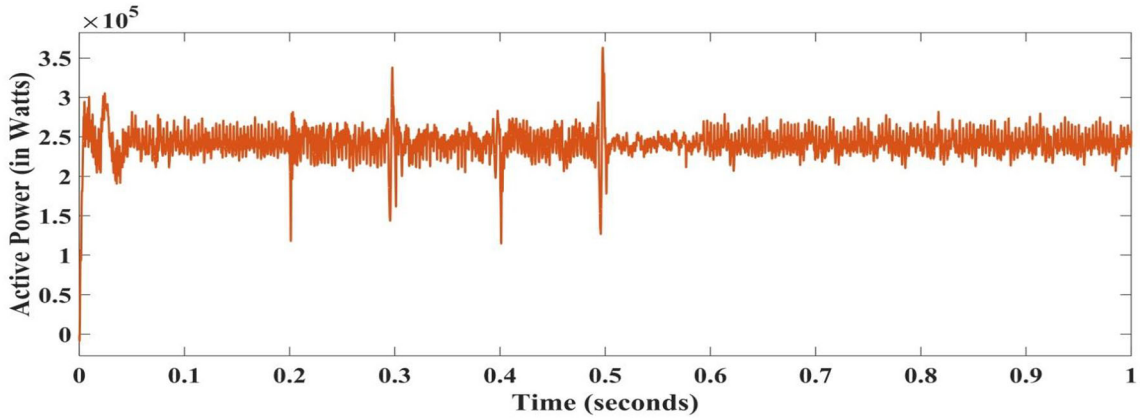

Fig. 12 Active power profile for VSM-based controller for sudden load changes

values. Both the controllers satisfy the IEEE standards and are well within the limits.

The voltage transients obtained from the VSM-based controller are considerably less than the PLL-based controller and hence show superior performance though both of them had voltage transients within the IEEE standards. Thus, for PV integrated grid system with 3 level multilevel converters, better performance is observed for VSM-based controller.

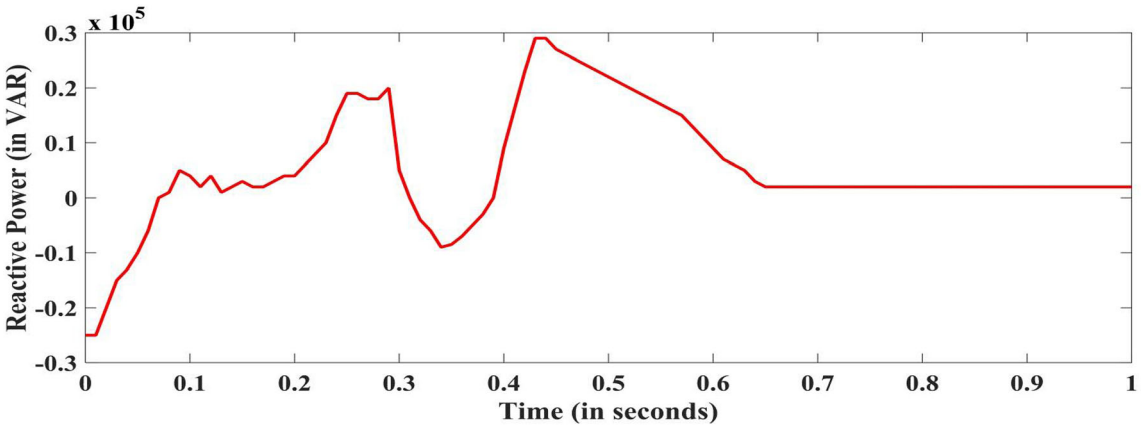

Fig. 13 Reactive power profile for VSM-based controller for sudden load changes

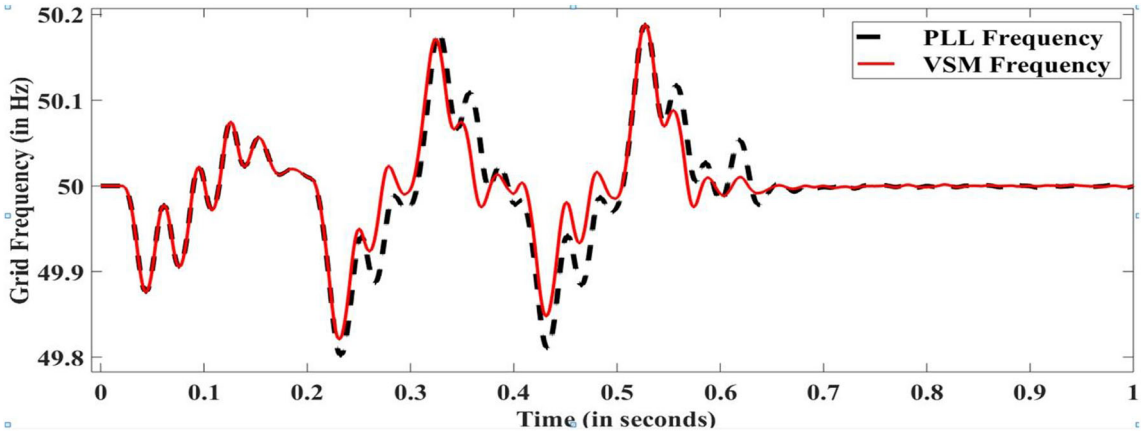

Fig. 14 Comparison of grid frequencies for both the controllers for sudden load changes

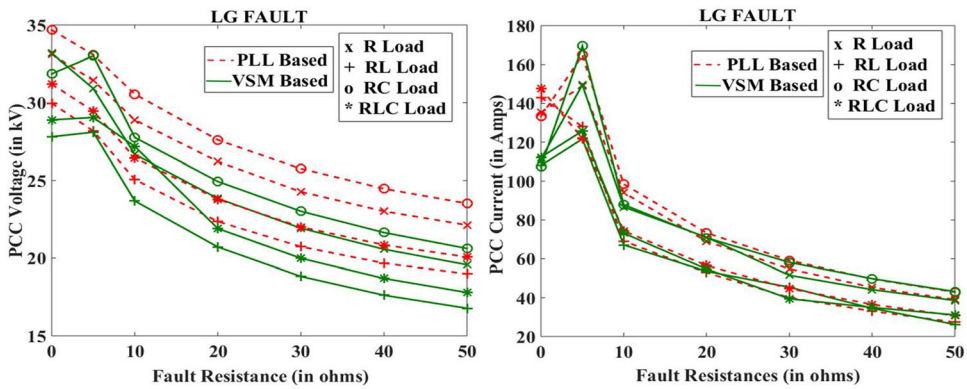

(a) (b)

Fig. 15 3-Level converter connected for both PLL and VSM-based controller for LG fault analysis at various load conditions. **a** PCC voltage profiles, **b** PCC current profiles

2. 5-Level Converter with PLL-Based and VSM-Based Controller

(i) LG Fault

Figure 18 depicts the nature of PCC current and PCC voltage when a 5-level converter is connected to both the controllers for simple LG fault for different fault resistance values. According to IEEE std. 1159, the voltage transients during fault conditions must be between 110 and 180% of nominal voltage [44]. Both the controllers satisfy the IEEE standards and are well within the limits.

(ii) LLG Fault

Figure 19 depicts the behaviour of PCC current and PCC voltage when a 5-level converter is connected to both

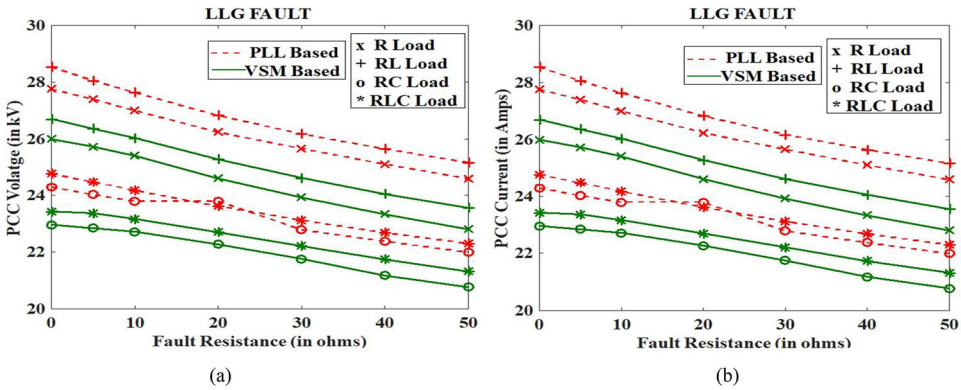

Fig. 16 3-Level converter connected for both PLL and VSM-based controller for LLG fault analysis at various load conditions. **a** PCC voltage profiles, **b** PCC current profiles

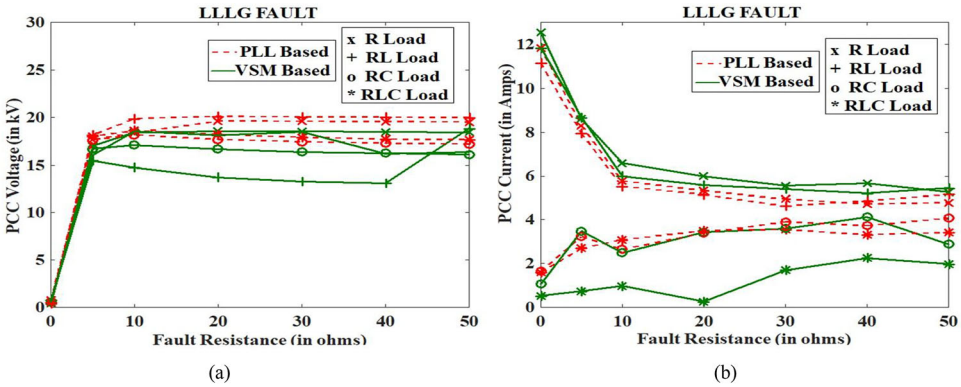

Fig. 17 3-Level converter connected for both PLL and VSM-based controller for LLLG fault analysis at various load conditions. **a** PCC voltage profiles, **b** PCC current profiles

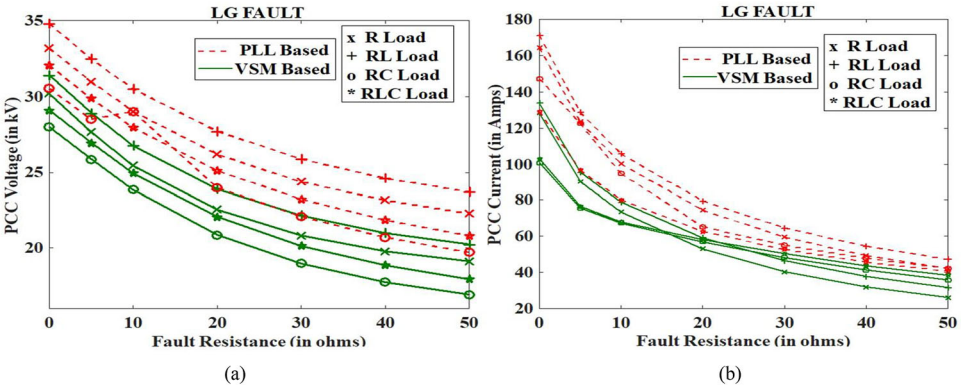

Fig. 18 5-Level converter connected for both PLL and VSM-based controller for LG fault analysis at various load conditions. **a** PCC voltage profiles, **b** PCC current profiles

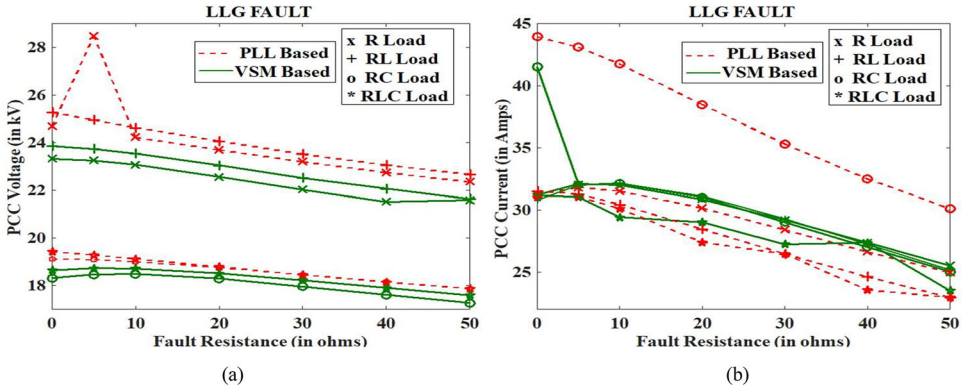

Fig. 19 5-Level converter connected for both PLL and VSM-based controller for LLG fault analysis at various load conditions. **a** PCC voltage profiles, **b** PCC current profiles

the controllers for LLG fault for different fault resistance values. Both the controllers satisfy the IEEE standards and are well within the limits.

(iii) LLLG Fault

Figure 20 shows the behaviour of PCC voltage and PCC current when a 5-level converter is connected to both the controllers for LLLG fault for different fault resistance values. Both the controllers satisfy the IEEE standards and are well within the limits.

For a 5-level multilevel inverter integrated with a PV integrated grid system, the VSM-based controller outperforms the PLL-based controller and has voltage transients that are well within the limits specified by IEEE std. 1159.

Fast Fourier Transform (FFT) Analysis

The Fast Fourier Transform (FFT) analysis is done on both the controller systems and their total harmonic distortion values are calculated. The FFT analysis is done for both 3 level and 5 level inverters with different loads. According to IEEE std. 519, if the bus or PCC voltage is $1\ \text{kV} < V < 69\ \text{kV}$, then the maximum permissible total harmonics distortion (THD) in the system must be 5% [45]. As, the study system used here in this simulation is of 25 kV, therefore, the THD level must be 5%.

1. 3-Level Inverter for PLL-Based and VSM-Based Controllers

Figures 21, 22, 23 and 24 shows the THD level of both PLL and VSM based controllers for 3-level inverter with load variations. It is observed that the THD level for VSM-based controllers is larger than the PLL-based controllers. However, the difference between their THD levels is very small. The THD levels for both of them are well within the IEEE std. 519 for harmonic limits. Hence, both of the controllers behave satisfactory for 3-level inverter integrated with the system.

(i) R-Load
(ii) RC-Load
(iii) RL-Load
(iv) RLC-Load

2. 5-Level Inverter for PLL-Based and VSM-Based Controller

Figures 25, 26, 27 and 28 shows the THD level of both PLL and VSM based controllers for 5-level inverter with load variations. The THD level for VSM-based controller is less than the PLL-based controller; however both the controllers' THD level is well within the limits specified by IEEE std. 519.

(i) **R-load**
(ii) **RC-load**
(iii) **RL-load**
(iv) **RLC load**

(d) Voltage Sag Compensation

At the start, the grid is not connected with the PV-STATCOM system. The test study bed is connected with a load of 25 MW and 15 MVAR during the time period of 0.3–0.6 s due to which voltage sag occurs. It is observed that the voltage at PCC is reduced from 20 to 4.7 kV which means voltage sag magnitude is 15.3 kV i.e. 76.5% of system voltage (i.e. 20 kV) is available as shown in Fig. 29.

Now, in order to compensate for the voltage sag that occurred due to overloading, the PV-STATCOM system is connected to the grid which acts as an auxiliary power supply as well as regulates the voltage as per the requirement. Figure 30 shows the PCC voltage compensated by a PV-STATCOM system which is being controlled by a PLL-based controller. It is observed that the PCC voltage is compensated to a magnitude of 17.8 kV. Figure 31 shows the PCC voltage compensated by a PV-STATCOM system which is being controlled by a VSM-based controller. It is

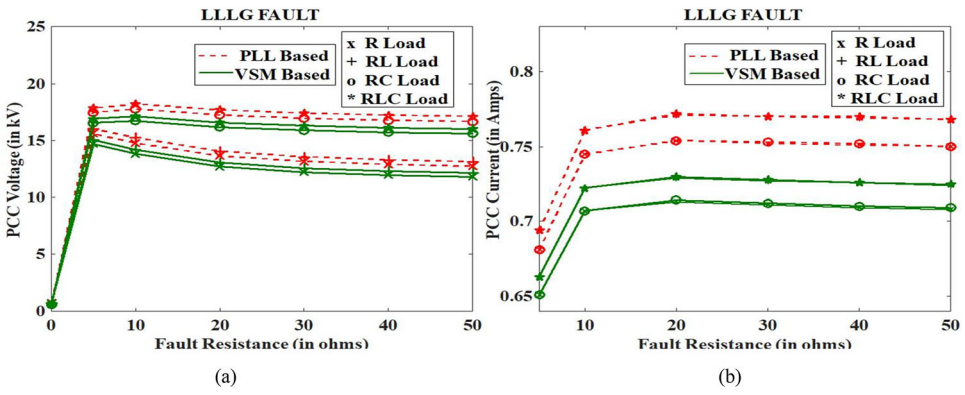

Fig. 20 5-Level converter connected for both PLL and VSM-based controller for LLLG fault analysis at various load conditions. **a** PCC voltage profiles, **b** PCC current profiles

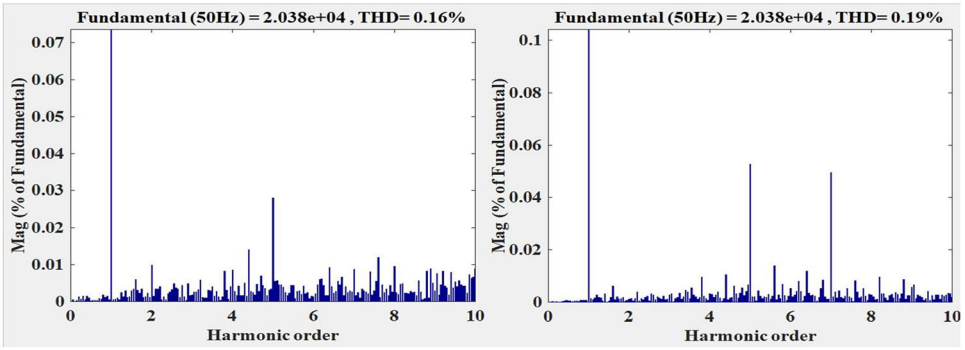

(a) (b)

Fig. 21 3-Level converter connected for both PLL and VSM-based controller for FFT analysis at R-load conditions. **a** PLL-based controller, **b** VSM-based controller

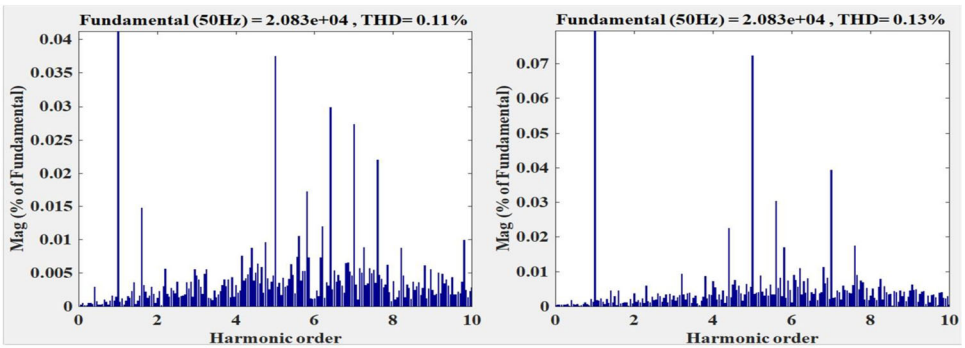

(a) (b)

Fig. 22 3-Level converter connected for both PLL and VSM-based controller for FFT analysis at RC-load conditions. **a** PLL-based controller, **b** VSM-based controller

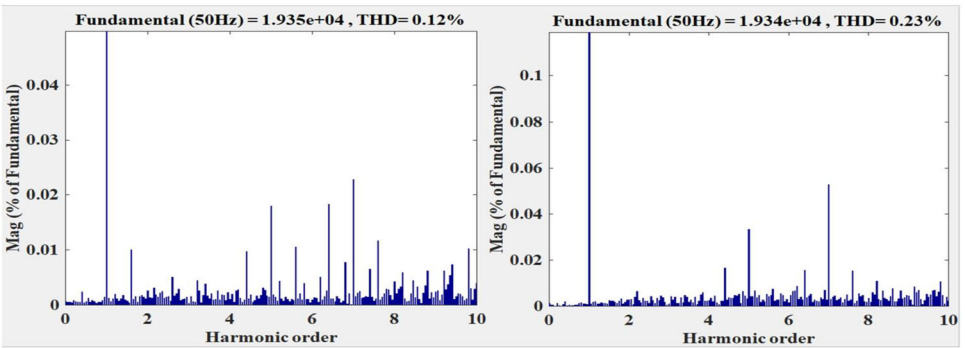

(a) (b)

Fig. 23 3-Level converter connected for both PLL and VSM-based controller for FFT analysis at RL-load conditions. **a** PLL-based controller, **b** VSM-based controller

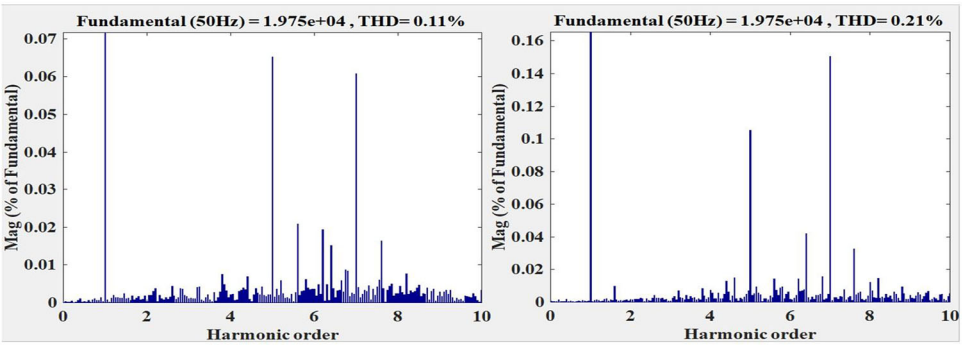

(a) (b)

Fig. 24 3-Level converter connected for both PLL and VSM-based controller for FFT analysis at RLC-load conditions. **a** PLL-based controller, **b** VSM-based controller

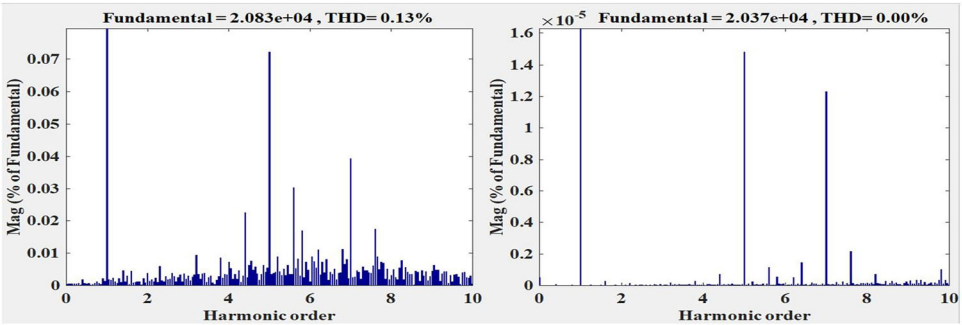

(a) (b)

Fig. 25 5-Level converter connected for both PLL and VSM-based controller for FFT analysis at R-load conditions. **a** PLL-based controller, **b** VSM-based controller

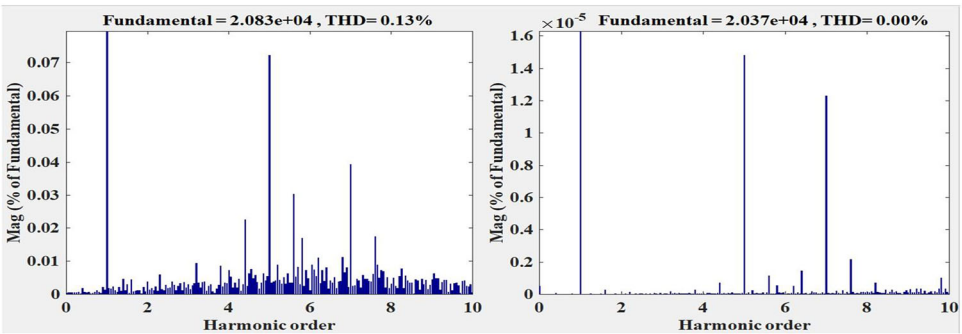

(a) (b)

Fig. 26 5-Level converter connected for both PLL and VSM-based controller for FFT analysis at RC-load conditions. **a** PLL-based controller, **b** VSM-based controller

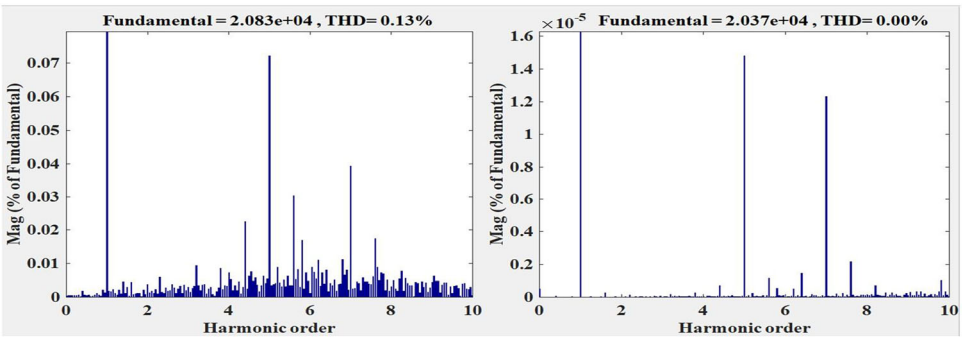

(a) (b)

Fig. 27 5-Level converter connected for both PLL and VSM-based controller for FFT analysis at RL-load conditions. **a** PLL-based controller, **b** VSM-based controller

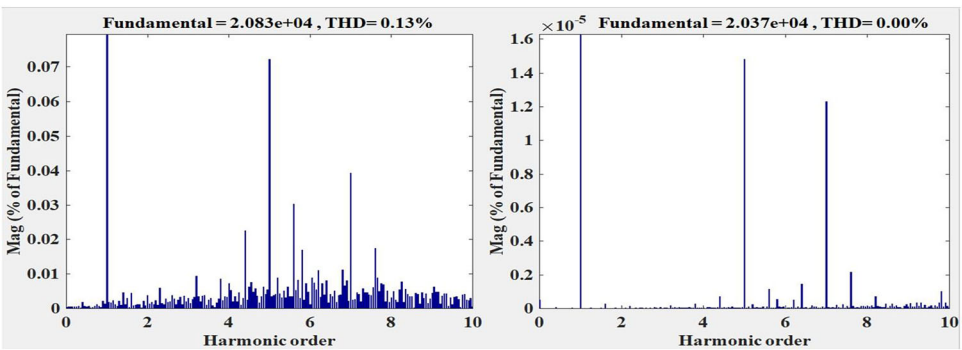

(a) (b)

Fig. 28 5-Level converter connected for both PLL and VSM-based controller for FFT analysis at RLC-load conditions. **a** PLL-based controller, **b** VSM-based controller

observed that the PCC voltage is compensated to a magnitude of 19.1 kV, which is almost equal to the rated PCC voltage. Figure 32 shows the reactive power injection during the voltage sag compensation process by the VSM based controller system.

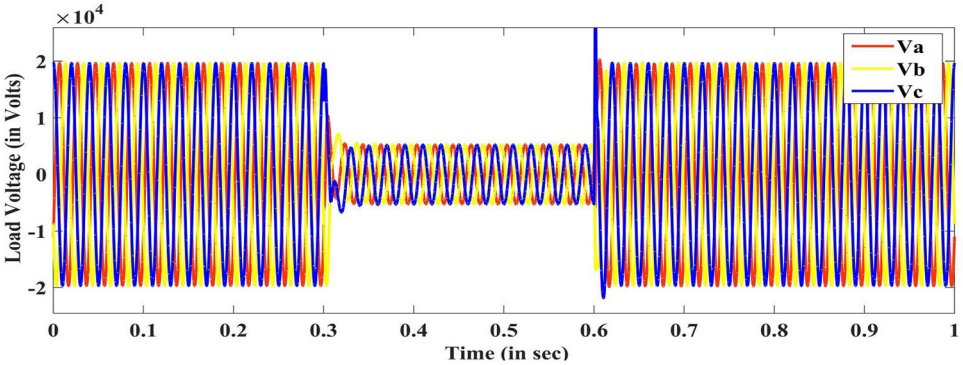

Fig. 29 Load voltage during 76.5% of sag in absence of PV-STATCOM

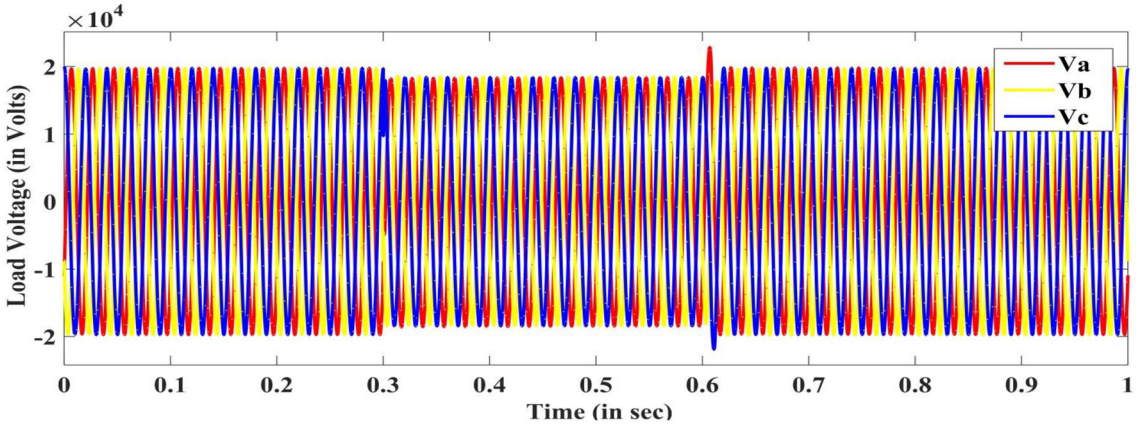

Fig. 30 Compensated voltage by PLL-based controller PV-STATCOM

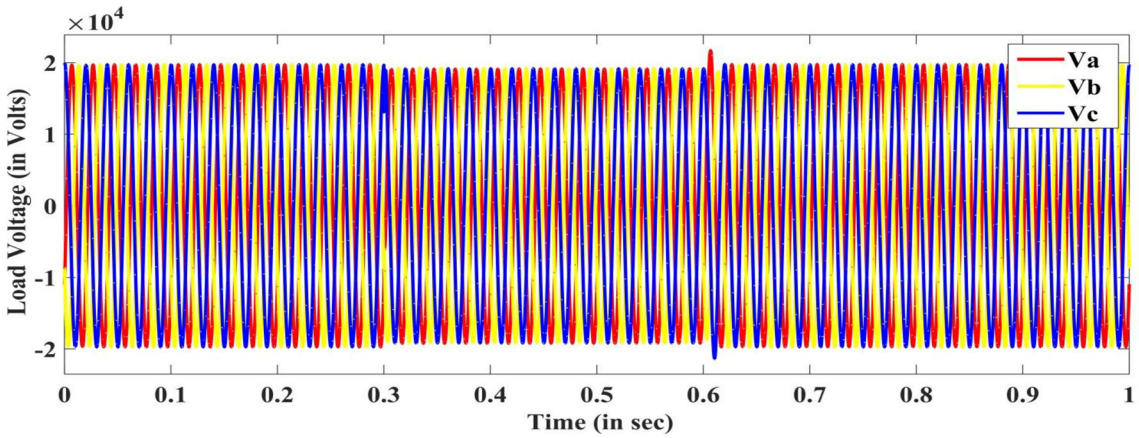

Fig. 31 Compensated voltage by VSM-based controller PV-STATCOM

5. Discussion

The study systems for both PLL-based and VSM-based controllers for PV-STATCOM were simulated for different sudden load magnitudes applied at constant time intervals and the voltage profiles were observed. It was evident from the results that the VSM-based controller showed more promising results than the PLL-based controller satisfying the IEEE std. 1547.2 which states that the permissible voltage deviation must be $\pm$ 5%.

The study system simulated voltage transients during different ground fault conditions at different fault resistance values and it was found that both the controllers had satisfactory performance within the limits set by IEEE std. 1159. However, the VSM-based controller showed comparatively less severe voltage transients than the PLL-based controller.

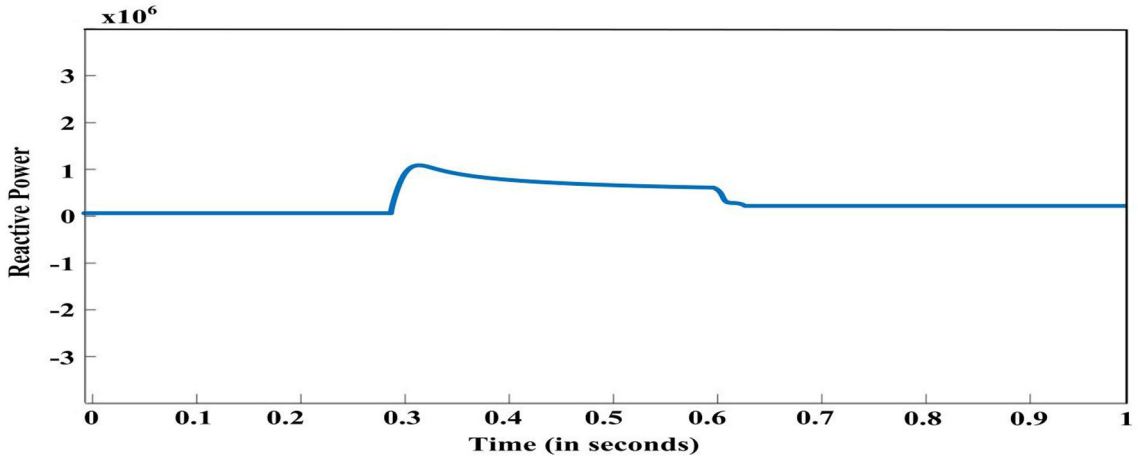

Fig. 32 Reactive power profile during voltage sag compensation

Table 1 % THD level for PLL-based and VSM-based controller for multilevel inverters

Loads	% THD Level			
	3-Level multilevel inverter		5-Level multilevel inverter	
	PLL	VSM	PLL	VSM
R	0.16	0.19	0.13	0
RC	0.11	0.13	0.13	0
RL	0.12	0.23	0.13	0
RLC	0.11	0.21	0.13	0

The study systems were also simulated for FFT analysis for various load conditions and both the controllers demonstrated considerable performance with THD well within the limit set by the IEEE std. 519. Table 1 shows the THD levels for PLL-based and VSM-based controllers for 3-level and 5-level multilevel inverters. The THD measured in the 3-level converter for the VSM-based controller was slightly higher than the THD measured in the PLL-based controller, but it was well within the limits. For the 5-level converter, the VSM-based controller showed very less THD levels in all load conditions than the PLL-based controller.

To prove the effectiveness of PV-STATCOM with VSM-based controller in all other aspects, the study system was also simulated for voltage sag compensation by overloading the system. It was observed that the voltage was compensated more effectively in the case of VSM-based controller than PLL-based controller for PV-STATCOM.

6. Conclusion

The PV-STATCOM concept of utilizing the grid connected inverter as STATCOM has been controlled by $d-q$ frame PLL-based and VSM-based controllers. The performance of these two controllers was evaluated under different contingencies, such as sudden loading and unloading of the power system, occurrence of faults with different loads, and FFT analysis for THD calculations. It was observed that the PLL-based control system had voltage transients surpassing boundaries imposed by IEEE standards for sudden load changes, while the VSM-based controller had voltage transients well within the defined range. It was also noted that both of these controllers showed satisfactory performance for fault and THD analysis remaining inside the limit set by IEEE standards. However, the VSM-based controller showed more promising results by having voltage transients and THD values well below the PLL-based controller for the 5-level converter. The voltage sag compensation ability of the VSM-based controller is better than the PLL-based controller for the PV-STATCOM system. It is therefore apparent from all the simulation comparison findings acquired that the VSM-based controller is more efficient and reliable than the PLL-based controller and makes it much more efficient if incorporated with 5-level inverter for PV-STATCOM.

Appendix

Table 2 Aavlgoh

Parameter	Ratings	Parameter	Ratings
PV cell (SunPower SPR-435NE-WHT-D PV module)		Rated angular frequency (ω_n)	$2\pi \times 50$ rad/s
PV array power	250 kW	*Transmission line parameters*	
PV voltage	481 V	Line resistance (R_{line})	0.37 mΩ/km
Open circuit voltage of cell (V_{oc})	85.6 V	Line inductance (L_{line})	0.09 mH/km
Short-circuit current of cell (I_{sc})	6.43 A	*Load ratings*	
Number of PV modules in series	7	Load active power, P_L	7 MW
Number of parallel strings	88	Load inductive reactive power, Q_L	5 MVAR
Sun Irradiance	1000 W/m^2	Load capacitive reactive Power, Q_C	2 MVAR
DC link voltage		*Controller parameters*	
Nominal DC link voltage (V_{dc})	464 V	Virtual inductance, L	50
DC link capacitance (C_{dc})	54.3 mF	Virtual resistor, R	$(0.1/\pi)$
Grid Parameters		Virtual angular momentum, M	$5 \times 10^{-3} \times \omega_n$
Grid voltage rms (V_g)	25 kV	Virtual damping factor, D	$1 \times \omega_n$
Grid rated power (P_g)	250 kW	*Other parameters*	
Nominal frequency (f)	50 Hz	PWM modulator switching frequency	1980 Hz
Grid X/R ratio	7	Sampling time (T_s)	5.05 μs

References

[1] M.G. Molina and P. E. Mercado, Modelling and control of grid-connected photovoltaic energy conversion system used as a dispersed generator, *2008 IEEE/PES Transmission and Distribution Conference and Exposition: Latin America, Bogota*, 2008, pp. 1–8, https://doi.org/10.1109/TDC-LA.2008.4641871.

[2] S. Huseinbegovic and B. Perunicic, New reactive power control concept for converter based renewable energy sources, *2011 19th Mediterranean Conference on Control & Automation (MED)*, Corfu, 2011, pp. 850–855, https://doi.org/10.1109/MED.2011.5982973.

[3] H. Magged, A.S. Nada, S. Abu-Zaid et al., Effects of waveforms distortion for household appliances on power quality. MAPAN, *34* (2019) 559–572.

[4] M. Bajaj and A.K. Singh, Grid integrated renewable DG systems: a review of power quality challenges and state-of-the-art mitigation techniques. Int J Energy Res, *44* (2019) 26–69.

[5] P.K. Madaria, M. Bajaj, S. Aggarwal and A.K. Singh, A grid-connected solar PV module with autonomous power management, *2020 IEEE 9th Power India International Conference (PIICON)*, Sonepat, India, 2020, pp. 1–6, https://doi.org/10.1109/PIICON49524.2020.9113065.

[6] N. Kumar and O. Buwa, A review on reactive power compensation of distributed energy system, *2020 7th International Conference on Smart Structures and Systems (ICSSS),* Chennai, India, 2020, pp. 1–6, https://doi.org/10.1109/ICSSS49621.2020.9202249.

[7] Mohan P. Thakre and Vijay S. Kale, An adaptive approach for three zone operation of digital distance relay with static var compensator using PMU. Electrical Power & Energy Systems, *77* (2016) 327–336.

[8] D. Koteswara Raju, B.S. Umre, M.P. Thakre et al., Fractional-order PI based UPFC damping controller to mitigate subsynchronous resonance. SpringerPlus, *5* (2016) 1–20.

[9] D.K. Raju, B.S. Umre, M.P. Thakre and V.S. Kale, Mitigation of subsynchronous oscillations with common controller based STATCOM and SSSC. J. Electr. Eng. Electron. Technol., *5* (2016) 735–744.

[10] K.V. Bhadane, M.S. Ballal, A. Nayyar, et al, A comprehensive study of harmonic pollution in large penetrated grid-connected wind farm, *MAPAN,* 2020

[11] A.R. Gidd, A.D. Gore, M.P. Thakre et.al, Modelling, analysis and performance of DSTATCOM for voltage sag mitigation in distribution system, *Proceedings of the 3rd IEEE International Conference on Trends in Electronics and Informatics (ICOEI 2019),* SCAD Clg. of Engg. & Tech., Tirunelveli, Tamil Nadu, India, 23–25 April 2019, CFP19J32-ART; ISBN: 978-1-5386-9439-8, pp. 366–371.

[12] M. Singh, V. Khadkikar, A. Chandra and R.K. Varma, Grid interconnection of renewable energy sources at the distribution level with power-quality improvement features. IEEE Transactions on Power Delivery, *26* (2011) 307–315. https://doi.org/10.1109/TPWRD.2010.2081384.

[13] R.K. Varma, V. Khadkikar and S.A. Rahman, 2016, *Utilization of Distributed Generator Inverters as STATCOM*, Patent No.: US 9325173B2, United States Patent

[14] R.K. Varma, V. Khadkikar and R. Seethapathy, Nighttime application of PV solar farm as STATCOM to regulate grid voltage. IEEE Transactions on Energy Conversion, *24* (2009) 983–985. https://doi.org/10.1109/TEC.2009.2031814.

[15] R.K. Varma, S.A. Rahman and T. Vanderheide, New control of PV solar farm as STATCOM (PV-STATCOM) for increasing grid power transmission limits during night and day. IEEE Transactions on Power Delivery, *30* (2015) 755–763. https://doi.org/10.1109/TPWRD.2014.2375216.

[16] R. Varma and E. Siavashi, PV-STATCOM—a new smart inverter for voltage control in distribution systems *2018 IEEE Power & Energy Society General Meeting (PESGM)*, Portland, OR, 2018, pp. 1–1. https://doi.org/10.1109/PESGM.2018.8586325.

[17] M. Azharuddin and S. R. Gaigowal, Voltage regulation by grid connected PV-STATCOM*, 2017 International Conference on Power and Embedded Drive Control (ICPEDC)*, Chennai, 2017, pp. 472–477. https://doi.org/10.1109/ICPEDC.2017.8081136.

[18] L. Aaltonen, M. Saukoski and K. Halonen, Design of clock generating fully integrated PLL using low frequency reference signal, *Proceedings of the 2005 European Conference on Circuit Theory and Design, 2005., Cork, Ireland,* 2005, pp. I/161–I/164, https://doi.org/10.1109/ECCTD.2005.1522935.

[19] O.V. Nos, E.E. Abramushkina and S.A. Kharitonov, Control design of fast response PLL for FACTS applications, *2019 International Ural Conference on Electrical Power Engineering (UralCon)*, Chelyabinsk, Russia, 2019, pp. 301–305, https://doi.org/10.1109/URALCON.2019.8877643.

[20] M.B. Delghavi and A. Yazdani, A control strategy for islanded operation of a distributed resource (DR) unit, *2009 IEEE Power & Energy Society General Meeting*, Calgary, AB, 2009, pp. 1–8, https://doi.org/10.1109/PES.2009.5275592.

[21] K.M.S.Y. Konara, M.L. Kolhe, W.G.C.A. Sankalpa, A.R. Wimucthi and D.D.M. Ranasinghe, Integration of DC power source in micro-grid using VSI with PLL technique, *2015 International conference on smart grid and clean energy technologies (ICSGCE)*, Offenburg, 2015, pp. 50–55, https://doi.org/10.1109/ICSGCE.2015.7454268.

[22] V.M. Najda and S.S. Alex, Performance analysis of synchronous reference frame based controller for grid interconnected microgrid, *2014 4th international conference on advances in computing and communications*, Cochin, 2014, pp. 255–259, https://doi.org/10.1109/ICACC.2014.68.

[23] Á. Ortega and F. Milano, Comparison of different PLL implementations for frequency estimation and control, *2018 18th international conference on harmonics and quality of power (ICHQP)*, Ljubljana, 2018, pp. 1–6, https://doi.org/10.1109/ICHQP.2018.8378935.

[24] L. Harnefors, 2011, *Control of a voltage source converter using synchronous machine emulation*, Patent No.: US 20110153113A1, United States Patent Application Publication

[25] S. D'Arco, J.A. Suul and O.B. Fosso, A virtual synchronous machine implementation for distributed control of power converters in smartgrids. Electric Power Systems Research, *122* (2015) 180–197.

[26] C. Li, R. Burgos, I. Cvetkovic, D. Boroyevich, L. Mili, and P. Rodrigues, Analysis and design of virtual synchronous machine based statcom controller, *Workshop on control and modeling for power electronics (COMPEL), IEEE Workshop on*, 2014

[27] M. Torres and L.A.C. Lopes, Virtual synchronous generator control in autonomous wind-diesel power systems, *2009 IEEE electrical power & energy conference (EPEC)*, Montreal, QC, 2009, pp. 1–6, https://doi.org/10.1109/EPEC.2009.5420953.

[28] H. Bevrani, T. Ise and Y. Miura, Virtual synchronous generators: a survey and new perspectives*", Electrical Power and Energy Systems*, 2013

[29] Q.C. Zhong and G. Weiss, Synchronoverters: inverters that mimic synchronous generator. IEEE Transactions on Industrial Electronics, *58* (2011) 4.

[30] Q. Zhong, P. Nguyen, Z. Ma and W. Sheng, Self-synchronized synchronverters: inverters without a dedicated synchronization unit. IEEE Transactions on Power Electronics, *29* (2014) 617–630. https://doi.org/10.1109/TPEL.2013.2258684.

[31] C. Li, R. Burgos, I. Cvetkovic, D. Boroyevich, L. Mili and P. Rodriguez, Evaluation and control design of virtual-synchronous-machine-based STATCOM for grids with high penetration of renewable energy, *2014 IEEE energy conversion congress and exposition (ECCE)*, Pittsburgh, PA, 2014, pp. 5652–5658, https://doi.org/10.1109/ECCE.2014.6954176.

[32] C. Li, R. Burgos, I. Cvetkovic, and D. Boroyevich, Active and reactive powerflow of a STATCOM with virtual synchronous machine control, *IEEE*, 2015

[33] H.P. Beck and R. Hesse, Virtual Synchronous Machine, *9th International conference on electrical power quality and utilisation, EPQU 2007*, pp 1–6

[34] M. Bajaj, S. Aggarwal and A. K. Singh, Power quality concerns with integration of RESs into the smart power grid and associated mitigation techniques, *2020 IEEE 9th Power India international conference (PIICON)*, Sonepat, India, 2020, pp. 1–6, https://doi.org/10.1109/PIICON49524.2020.9113008.

[35] N. Kumar, O.N. Buwa and M.P. Thakre, Virtual synchronous machine based PV-STATCOM Controller, *2020 IEEE 1st international conference on smart technologies for power, energy and control (STPEC),* Nagpur, 2020, pp. 1–6, https://doi.org/10.1109/STPEC49749.2020.9297718.

[36] K. Roopa, P. Jugge and S.T. Kalyani, A new 15-level inverter configuration with fault tolerant capability for PV applications, *2017 IEEE international conference on power, control, signals and instrumentation engineering (ICPCSI)*, Chennai, India, 2017, pp. 1830–1835, https://doi.org/10.1109/ICPCSI.2017.8392031.

[37] G. Revana and V.R. Kota, Closed loop artificial neural network controlled PV based cascaded boost five-level inverter system, *2017 International conference on green energy and applications (ICGEA)*, Singapore, 2017, pp. 11–17, https://doi.org/10.1109/ICGEA.2017.7925447.

[38] K. Singh, P. Swathi and M.U. Reddy, Performance analysis of PV inverter in microgrid connected with PV system employing ANN control, *2014 international conference on green computing communication and electrical engineering (ICGCCEE)*, Coimbatore, India, 2014, pp. 1–6, https://doi.org/10.1109/ICGCCEE.2014.6922390.

[39] D.S. Maurya, P.D. Jadhav, R.S. Joshi, R.R. BendkhaLe and M.P. Thakre, A detailed comparative analysis of different multipulse and multilevel topologies for STATCOM, *2020 International conference on electronics and sustainable communication systems (ICESC),* Coimbatore, India, 2020, pp. 1112–1117, https://doi.org/10.1109/ICESC48915.2020.9155708.

[40] V.V. Hadke and M.P. Thakre, Integrated multilevel converter topology for speed control of SRM drive in plug in-hybrid electric vehicle, *Proceedings of the 3rd IEEE international conference on trends in electronics and informatics (ICOEI 2019),* SCAD Clg. of Engg. & Tech., Tirunelveli, Tamil Nadu, India, 23–25 April 2019, CFP19J32-ART; ISBN: 978-1-5386-9439-8, pp. 1013–1018

[41] N.R. Rode, S.R. Gaigowal, A.A. Dutta and P.A. Meshram, Multilevel inverter based PV-STATCOM, *2018 3rd IEEE international conference on recent trends in electronics, information and communication technology (RTEICT)*, Bangalore, India, 2018, pp. 2173–2177, https://doi.org/10.1109/RTEICT42901.2018.9012407.

[42] N.R. Rode, S.R. Gaigowal and P.S. Patil, Cascaded H-bridge inverter based PV-STATCOM, *2018 International conference on smart electric drives and power system (ICSEDPS)*, Nagpur, India, 2018, pp. 99–104, https://doi.org/10.1109/ICSEDPS.2018.8536072.

[43] "IEEE Application Guide for IEEE Std. 1547(TM), IEEE standard for interconnecting distributed resources with electric power systems, *in IEEE Std. 1547.2–2008*, pp.1–217, 15 April 2009, https://doi.org/10.1109/IEEESTD.2008.4816078.

[44] "IEEE recommended practice for monitoring electric power quality, *in IEEE Std. 1159–2019 (Revision of IEEE Std. 1159–2009)*, pp.1–98, 2019, https://doi.org/10.1109/IEEESTD.2019.8796486.

[45] "IEEE recommended practice and requirements for harmonic control in electric power systems," *in IEEE Std. 519–2014 (Revision of IEEE Std. 519–1992),* pp.1–29, 2014, https://doi.org/10.1109/IEEESTD.2014.6826459.